Malaya Journal of Matematik, Vol. 8, No. 3, 730-737, 2020

https://doi.org/10.26637/MJM0803/0001

The study of effects of surface tension, magnetic field and non-uniform salinity gradients on the onset of double diffusive convection in composite system

R. Sumithra [1] and B. Komala [2*]

Abstract

The effects of surface tension, magnetic field and basic non - uniform salinity gradients on the onset of double diffusive convection is studied analytically in composite system comprising an incompressible, two component, electrically conducting fluid lying above a saturated porous layer of the same fluid in the presence of vertical magnetic field imposed. The governing partial differential equations are solved by the method of regular perturbation. The upper boundary of the fluid layer is free and the lower boundary of the porous layer is rigid, insulated to heat and mass. The fluid flow in porous layer is governed by the Darcy-Brinkman equation. The critical Rayleigh number which exhibits the stability of the system is accomplished for piece wise linear salting below, desalting above and step function salinity gradients. We have figured out that by increasing Darcy number, due to the presence of magnetic field the convection is accelerated in all the three non uniform salinity gradients considered.

Keywords

Double diffusion convection, Surface tension, Magnetic field, Salinity gradients, Regular perturbation method, Darcy-Brinkman model.

AMS Subject Classification

76-XX, 76Rxx, 76Sxx.

[1] *Department of Mathematics, Government Science College, N. T Road, Bangalore-560001, Karnataka, India.*

[2] *Department of Mathematics, Dayananda Sagar University, Bangalore-560068, Karnataka, India.*

***Corresponding author**: sumitra_diya@yahoo.com; [2] komala550@gmail.com

Article History: Received **18** February **2020**; Accepted **29** April **2020**

Contents

1. Introduction

Convective instability in a composite layer may occur either due to buoyancy forces or surface tension variations in the presence of temperature and/or concentration gradients or combined buoyancy and surface tension forces. In this paper, we study the natural convection driven by both thermal and solutal buoyancy forces with an externally imposed magnetic field in superposed porous layer over which lies a layer of same fluid. Convective flow driven by both buoyancy and surface tension play an important role in science, engineering and technology, especially in solidification, crystals growth and in materials processing.

The study of convective flows driven by surface tension which is also known as Marangoni convection was initiated by Pearson (1958) with the assumptions of infinitesimally small amplitude analysis. He considered non - deformable free surface and no-slip boundary condition at the bottom. He showed that the variations in the surface tension at the free surface due to temperature gradients could induce motion within the fluid. Nield (1977) investigated the thermal stability of superposed porous and fluid layers by using linear stability analysis for an empirical interfacial condition at the fluid-porous interface suggested by Beavers and Joseph. Chen et al., (1991) discussed the onset of buoyancy-driven convection due to heating from below in a system consisting of a fluid layer overlying a porous layer with anisotropic permeability and thermal diffusivity. Convective instability in a liquid saturated porous layer due to surface tension and/or buoyancy forces has also been investigated by Hennenberg, M.Z et al.,(1997), N. Rudraiah et al (1998) and references therein . Shivakumara et al. (2006) studied the onset of Marangoni convection in a composite porous-layer system and the Beavers-Joseph slip condition is used at the interface and the Darcy law is employed to describe the flow in the porous medium. Shivakumara et al. (2011) investigated the criterion for the onset of surface tension-driven convection in the presence of temperature gradients in a two-layer system comprising a fluid saturated anisotropic porous layer over which lies a layer of fluid. The lower rigid surface is assumed to be insulated to temperature perturbations, while at the upper non-deformable free surface a general thermal condition is invoked. Both the Beavers–Joseph and the Jones conditions have been used at the interface to know their preference and prominence in the study of the problem. The resulting eigenvalue problem is solved exactly and also by regular perturbation technique when both the boundaries are insulating to temperature perturbations.

The purpose of the present work is to derive the analytical expression for critical Rayleigh number for the onset of convection for basic non - uniform salinity gradients and hence the influence of various physical parameter on the stability of the system through graphical interpretations.

2. Problem Configuration

The composite system with free top layer and rigid bottom layer is considered. At the interface, the velocity, shear stress, normal stress, heat, heat flux, mass and mass flux are presumed to be continuous with magnetic field along vertical z - axis. The governing equations following the laws of conservation of mass, solenoidal property of magnetic field, momentum, heat and salinity, with Boussinesq approximation are as below
For region-1,

$$\nabla\cdot\vec{q} = 0 \quad (2.1)$$
$$\nabla\cdot\vec{H} = 0 \quad (2.2)$$

$$\rho_0\left[\frac{\partial\vec{q}}{\partial t}+(\vec{q}\cdot\nabla)\vec{q}\right] = -\nabla P+\mu\nabla^2\vec{q}+\rho g\hat{k}+\mu_p\left(\vec{H}\cdot\nabla\right)\vec{H} \quad (2.3)$$

$$\frac{\partial T}{\partial t}+(\vec{q}\cdot\nabla)T=\kappa\nabla^2 T \quad (2.4)$$
$$\frac{\partial C}{\partial t}+(\vec{q}\cdot\nabla)C=D\nabla^2 C \quad (2.5)$$
$$\frac{\partial\vec{H}}{\partial t}=\nabla\times\vec{q}\times\vec{H}+\nu_m\nabla^2\vec{H} \quad (2.6)$$
$$\rho=\rho_0\left[1-\alpha_t(T-T_0)+\alpha_s(C-C_0)\right] \quad (2.7)$$

and for region-2,

$$\nabla_m\cdot\vec{q}_m = 0 \quad (2.8)$$
$$\nabla_m\cdot\vec{H} = 0 \quad (2.9)$$

$$\rho_0\left[\frac{1}{\varepsilon}\frac{\partial\vec{q}_m}{\partial t}+\frac{1}{\varepsilon^2}(\vec{q}_m\cdot\nabla_m)\vec{q}_m\right]=-\nabla_m P_m+\mu\nabla^2\vec{q}_m-\frac{\mu}{K}\vec{q}_m-\rho_m g\hat{k}+\mu_p\left(\vec{H}\cdot\nabla_m\right)\vec{H}+\frac{\vec{q}_m}{\sqrt{K}}C_b\left|\vec{q}_m\right|\vec{q}_m \quad (2.10)$$

$$A\frac{\partial T_m}{\partial t}+(\vec{q}_m\cdot\nabla_m)T_m=\kappa_m\nabla_m^2 T_m \quad (2.11)$$
$$\varepsilon\frac{\partial C_m}{\partial t}+(\vec{q}_m\cdot\nabla_m)C_m=D_m\nabla_m^2 C_m \quad (2.12)$$
$$\varepsilon\frac{\partial\vec{H}}{\partial t}=\nabla_m\times\vec{q}_m\times\vec{H}_m+\nu_{em}\nabla_m^2\vec{H}_m \quad (2.13)$$
$$\rho_m=\rho_0\left[1-\alpha_{tm}(T_m-T_0)+\alpha_{sm}(C_m-C_0)\right] \quad (2.14)$$

The basic steady state is assumed to the quiescent, since the stability of the basic solution is at interest, the basic equations are then perturbed by considering infinitesimal perturbations. The perturbed variables are then rendered dimensionless and subjected to normal mode analysis. An Eigen value problem with the subsequent ordinary differential equations is attained by presuming that the principle of exchange of instabilities holds good for composite system.
In region-1

$$\left(D^2-a^2\right)^2 W=Ra^2\Theta-R_s a^2\Sigma-QD^2W \quad (2.15)$$
$$\left(D^2-a^2\right)\Theta+W=0 \quad (2.16)$$
$$\tau\left(D^2-a^2\right)\Sigma+Wg(z)=0 \quad (2.17)$$

In region-2

$$\left(\left(D_m^2-a_m^2\right)\hat{\mu}\beta^2-1\right)\left(D_m^2-a_m^2\right)W_m=(R_m\Theta_m-R_{sm}\Sigma_m)a_m^2-Q_mD_m^2W_m \quad (2.18)$$

$$\left(D_m^2-a_m^2\right)\Theta_m+W_m=0 \quad (2.19)$$
$$\tau_{pm}\left(D_m^2-a_m^2\right)\Sigma_m+W_m g_m(z_m)=0 \quad (2.20)$$

3. Boundary conditions

To obtain the solution of the above ordinary differential equation, the following boundary conditions are used
At $z_m = d_m$ the boundary conditions are

$$w_m = 0, \quad \frac{\partial w_m}{\partial z_m} = 0, \quad \frac{\partial T_m}{\partial z_m} = 0, \quad \frac{\partial S_m}{\partial z_m} = 0.$$

At $z = d$ the boundary conditions are,

$$\frac{\partial^2 w}{\partial z^2} + Ma^2\theta + M_s a^2 S = 0,$$
$$w = 0, \quad \frac{\partial \theta}{\partial z} = 0, \quad \frac{\partial S}{\partial z} = 0$$

At $z = 0$ and $z_m = 0$ (following Nield (1977)),

$$w = w_m, \quad \frac{\partial w}{\partial z} = \frac{\partial w_m}{\partial z_m}, \quad T = T_m,$$
$$\kappa\frac{\partial T}{\partial z} = \kappa_m \frac{\partial T_m}{\partial z_m}, \quad S = S_m, \quad \kappa\frac{\partial S}{\partial z} = \kappa_{sm}\frac{\partial S_m}{\partial z_m},$$
$$\mu\left(3\nabla_2^2 + \frac{\partial^2}{\partial z^2}\right)\frac{\partial w}{\partial z} = -\frac{\mu_m}{K}\frac{\partial w_m}{\partial z_m} +$$
$$\mu_m\beta^2\left(3\nabla_{2m}^2 + \frac{\partial^2}{\partial z_m^2}\right)\frac{\partial w_m}{\partial z_m},$$
$$\mu\left(-\frac{\partial^2 w}{\partial z^2} + \nabla_2^2 w\right) = \mu_m\left(-\frac{\partial^2 w_m}{\partial z_m^2} + \nabla_{2m}^2 w_m\right)$$

The above boundary conditions are made dimensionaless and exposed to Normal mode expansion which are as below,

$$D^2W(1) + Ma^2\Theta(1) + M_s a^2 S(1) = 0,$$
$$W(1) = 0, \quad D\Theta(1) = 0, \quad W_m(0) = 0,$$
$$D_m W_m(0) = 0, \quad D_m\Theta_m(0) = 0,$$
$$D_m S_m(0) = 0, \quad DS(0) = D_m S_m(1),$$
$$\hat{T}W(0) = W_m(1), \quad \hat{T}\hat{d}DW(0) = D_m W_m(1),$$
$$\hat{T}\hat{d}^2\left(D^2 + a^2\right)W(0) = \hat{\mu}\left(D_m^2 + a_m^2\right)W_m(1),$$
$$\Theta(0) = \hat{T}\Theta_m(1), \quad D\Theta(0) = D_m\Theta_m(1),$$
$$DS(1) = 0, \quad S(0) = \hat{S}S_m(1),$$
$$\hat{T}\hat{d}^2\beta^2\left(D^3W(0) - 3a^2DW(0)\right) =$$
$$D_m W_m(1)\left(\hat{\mu}\beta^2 D_m^2 W_m(1) - 1\right) - 3\hat{\mu}\beta^2 a_m^2 D_m W_m(1).$$

4. Solution by Regular Perturbation technique

For the constant heat and mass flux boundaries, convection sets in at small values of horizontal wave number a, accordingly, we expand

$$\begin{bmatrix} W \\ \theta \\ S \end{bmatrix} = \sum_{j=0}^{\infty} a^{2j}\begin{bmatrix} W_j \\ \Theta_j \\ S_j \end{bmatrix} \tag{4.1}$$

$$\begin{bmatrix} w_m \\ \theta_m \\ S_m \end{bmatrix} = \sum_{j=0}^{\infty}\left(\hat{d}a\right)^{2j}\begin{bmatrix} W_{mj} \\ \theta_{mj} \\ S_{mj} \end{bmatrix} \tag{4.2}$$

Substituting equation (4.1) and (4.2) in equations (2.15) to (2.20) we get the following leading order equations in a^2 as,
For the fluid layer

$$D^4W_0 - QD^2W_0 = 0 \tag{4.3}$$
$$D^2\Theta_0 + W_0 = 0 \tag{4.4}$$
$$\tau D^2\Sigma_0 + W_0 g(z) = 0 \tag{4.5}$$

For the porous layer,

$$\hat{\mu}\beta^2 D_m^4 W_{m0} - D_m^2 W_{m0} - Q_m D_m^2 W_{m0} = 0 \tag{4.6}$$
$$D_m^2\Theta_{m0} + W_{m0} = 0 \tag{4.7}$$
$$\tau_m D_m^2\Sigma_{m0} + W_{m0} g_m(z_m) = 0 \tag{4.8}$$

The boundary conditions to solve the above first order equations are,

$$W_0(1) = 0, \; D^2W_0(1) = 0, \; D\Theta_0(1) = 0,$$
$$DS_0(1) = 0, \quad \hat{T}\hat{d}DW_0(0) = D_m W_{m0}(1),$$
$$\hat{T}\hat{d}^2 D^2 W_0(0) = \hat{\mu} D_m^2 W_{m0}(1),$$
$$D\Theta_0(0) = D_m\Theta_{m0}(1),$$
$$S_0(0) = \hat{S}S_{m0}(1), \quad DS_0(0) = D_m S_{m0}(1),$$
$$\hat{T}\hat{d}^3\beta^2 D^3 W_0(0) = -D_m W_{m0}(1) + \hat{\mu}\beta^2 D_m^3 W_{m0}(1),$$
$$\hat{T}W_0(0) = W_{m0}(1), \quad D_m S_{m0}(0) = 0,$$
$$\Theta_0(0) = \hat{T}\Theta_{m0}(1), \quad D_m\Theta_{m0}(0) = 0,$$
$$W_{m0}(0) = 0, \; D_m W_{m0}(0) = 0, \quad .$$

With an arbitrary factor, the solutions for zero order equations are:

$$W_0(z) = 0, \quad S_0(z) = \hat{S}, \quad \Theta_0(z) = \hat{T},$$
$$W_{m0}(z) = 0, \quad S_{m0}(z) = 1, \quad \Theta_{m0}(z) = 1.$$

The equations at first order in a^2 are
For the fluid layer

$$D^4W_1 - QD^2W_1 - R\hat{T} + R_s\hat{S} = 0 \tag{4.9}$$
$$D^2\Theta_1 - \hat{T} + W_1 = 0 \tag{4.10}$$
$$\tau D^2\Sigma_1 - \tau\hat{S} + W_1 g(z) = 0 \tag{4.11}$$

For the porous layer,

$$\hat{\mu}\beta^2 D_m^4 W_{m1} - D_m^2 W_{m1} - Q_m\beta^2 D_m^2 W_{m1} - R_m + R_{sm} = 0 \tag{4.12}$$

$$D_m^2\Theta_{m1} - 1 + W_{m1} = 0 \tag{4.13}$$
$$\tau_m D_m^2\Sigma_{m1} - \tau_m + W_{m1} g_m(z_m) = 0 \tag{4.14}$$

The corresponding boundary conditions are,

$$
\begin{aligned}
&D^2W_1(1)+M\Theta_0(1)+M_sS_0(1)=0,\\
&D\Theta_1(1)=0,\quad DS_1(1)=0, W_{m1}(0)=0,\\
&W_1(1)=0,\quad D_mW_{m1}(0)=0,\\
&D_m\Theta_{m1}(0)=0,\quad D_mS_{m1}(0)=0,\\
&\hat{T}W_1(0)=\hat{d}^2W_{m1}(1),\quad \Theta_1(0)=\hat{T}\hat{d}^2\Theta_{m1}(1),\\
&\hat{T}\hat{d}DW_1(0)=\hat{d}^2D_mW_{m1}(1),\\
&\hat{T}\hat{d}^2D^2W_1(0)=\hat{\mu}D_m^2W_{m1}(1)\hat{d}^2,\\
&DS_1(0)=\hat{d}^2D_mS_{m1}(1),\\
&D\Theta_1(0)=\hat{d}^2D_m\Theta_{m1}(1),\ S_1(0)=\hat{S}\hat{d}^2S_{m1}(1),\\
&\hat{T}\hat{d}^3\beta^2D^3W_1(0)=-\hat{d}^2D_mW_{m1}(1)\\
&+\hat{\mu}\beta^2\hat{d}^2D_m^3W_{m1}(1).
\end{aligned}
$$

The solutions of the Eqs.(4.9) and (4.12) give W_1 and W_{m1} respectively which are important in obtaining the Eigen values and are found to be,

$$W_1(z)=a_1+a_2z+a_5-\left(R\hat{T}-R_s\hat{S}\right)\frac{z^2}{2Q} \tag{4.15}$$

$$W_{m1}(z_m)=b_1+b_2z_m+b_5-(R_m-R_{sm})\frac{{z_m}^2}{2(1+Q_m\beta^2)} \tag{4.16}$$

where $\zeta=\sqrt{\dfrac{1+Q_m\beta^2}{\hat{\mu}\beta^2}}$ and $a_1, a_2, a_3,\ a_4$ and b_1, b_2, b_3, b_4 are found using the velocity boundary conditions as below

$$
\begin{aligned}
&b_1=\frac{(\Delta_1\Delta_6-\Delta_3\Delta_5)}{(\Delta_2\Delta_4-\Delta_1\Delta_5)},\quad b_2=\frac{\zeta(\Delta_3\Delta_4-\Delta_1\Delta_6)}{(\Delta_2\Delta_4-\Delta_1\Delta_5)},\\
&b_3=-b_1,\quad b_4=-b_2/\zeta,\\
&b_5=b_3cosh(\zeta z_m)+b_4sinh(\zeta z_m),\\
&a_1=b_3\left(\frac{-\mu\zeta^2cosh\zeta}{\hat{T}Q}+\frac{\hat{d}^2(cosh\zeta-1)}{\hat{T}}\right)-\frac{2R}{Q}\\
&+b_4\left(\frac{-\mu\zeta^2sinh\zeta}{\hat{T}Q}+\frac{\hat{d}^2(sinh\zeta-\zeta)}{\hat{T}}\right)\\
&-R_m\left(\frac{2\mu}{\hat{T}Q}+\frac{\hat{d}^2}{\hat{T}}\right),\quad C=\frac{2R_m}{\hat{T}\hat{d}\beta^2Q\sqrt{Q}},\\
&a_3=\frac{2R}{Q}+\frac{\hat{\mu}}{\hat{T}Q}\left[b_3\zeta^2cosh\zeta+b_4\zeta^2sinh\zeta-2R_m\right],\\
&a_2=\left(\frac{\hat{d}sinh\zeta}{\hat{T}}-A\sqrt{Q}\right)b_3+\\
&\left(\frac{\hat{d}cosh\zeta-1}{\hat{T}}-B\sqrt{Q}\right)b_4-C\sqrt{Q}+\frac{2\hat{d}R_m}{\hat{T}},\\
&a_4=b_3A+b_4B+C,\\
&a_5=sech\left(\sqrt{Q}z\right)\left(a_3+a_4tanh\left(\sqrt{Q}z\right)\right),\\
&A=\frac{\zeta\left(\hat{\mu}\beta^2\zeta^2-1\right)sinh\zeta}{\hat{T}\hat{d}\beta^2Q\sqrt{Q}},\\
&B=\frac{\zeta\left(\hat{\mu}\beta^2\zeta^2cosh\zeta-cosh\zeta+1\right)}{\hat{T}\hat{d}\beta^2Q\sqrt{Q}}.
\end{aligned}
$$

4.1 Solvability condition

The solvability condition is obtained by using equations (4.10), (4.11), (4.13) and (4.14) with their respective boundary conditions as below

$$
\begin{aligned}
&\int_0^1 W_1dz+\tau_{pm}\int_0^1 W_1g(z)dz+\hat{d}^2\int_0^1 W_{m1}dz_m+\\
&\tau\hat{d}^2\int_0^1 W_{m1}g_m(z_m)dz_m=\hat{T}+\hat{d}^2+\tau\,\tau_{pm}\left(\hat{S}+\hat{d}^2\right)
\end{aligned} \tag{4.17}
$$

By substituting expressions for W_m and W_{m1} in equation (4.17) we obtain an expression for critical Rayleigh number for different basic salinity profiles which are as discussed below.

4.2 Piecewise linear salting below salinity profile :

For this case following Currie (1967),

$$
g(z)=\begin{cases}\varepsilon^{-1}, & 0\le z\le\varepsilon\\ 0, & \varepsilon\le z\le 1\end{cases},
$$

$$
g_m(z_m)=\begin{cases}\varepsilon_m^{-1}, & 0\le z_m\le\varepsilon_m\\ 0, & \varepsilon_m\le z_m\le 1\end{cases}
$$

For this profile, the critical Rayleigh number is established from (4.17) and is accessed as $R_{c4}=\dfrac{\kappa\,\Delta_{37}}{\hat{T}\,\Delta_{38}}$, where $\delta's$ are given by

$$
\begin{aligned}
&\delta_1=sinh\sqrt{Q}+\frac{\tau_{pm}sinh\left[\varepsilon\sqrt{Q}\right]}{\varepsilon},\\
&\delta_2=cosh\sqrt{Q}-1+\frac{\tau_{pm}\left(cosh\left[\varepsilon\sqrt{Q}\right]-1\right)}{\varepsilon},\\
&\delta_3=sinh\zeta+\frac{\tau sinh\left[\zeta\varepsilon_m\right]}{\varepsilon_m},\\
&\delta_4=cosh\zeta-1+\frac{\tau\left(cosh\left[\zeta\varepsilon_m\right]-1\right)}{\varepsilon_m},\\
&\delta_5=\frac{\delta_3}{\zeta}-1-\tau,\quad \delta_6=\frac{\delta_4}{\zeta}-\frac{\zeta}{2}(1+\tau\varepsilon_m),
\end{aligned}
$$

$$\delta_7=\left(\frac{\delta_2}{\sqrt{Q}}\right)\Delta_{27}+\hat{d}^2\delta_5\Delta_{16}+\hat{d}^2\delta_6\Delta_{17}$$
$$-\hat{d}^2\left(\frac{1+\varepsilon_m^2\tau}{3}\right),$$
$$\delta_8=\left(\frac{\delta_2}{\sqrt{Q}}\right)\Delta_{31}-\hat{d}^2\delta_5\Delta_{18}+\hat{d}^2\delta_6\Delta_{19},$$
$$\delta_9=\left(\frac{\delta_2}{\sqrt{Q}}\right)\Delta_{23}-\hat{d}^2\delta_5\Delta_{14}+\hat{d}^2\delta_6\Delta_{15}-$$
$$\left(\frac{1+\varepsilon\tau_{pm}}{3}\right),$$
$$\Delta_{34}=(1+\tau_{pm})\Delta_{24}+\left(\frac{1+\varepsilon\tau_{pm}}{2}\right)\Delta_{25}+$$
$$\left(\frac{\delta_1}{\sqrt{Q}}\right)\Delta_{26}+\delta_7,$$
$$\Delta_{35}=(1+\tau_{pm})\Delta_{28}+\left(\frac{1+\varepsilon\tau_{pm}}{2}\right)\Delta_{29}+$$
$$\left(\frac{\delta_1}{\sqrt{Q}}\right)\Delta_{30}+\delta_8,$$
$$\Delta_{36}=(1+\tau_{pm})\Delta_{20}+\left(\frac{1+\varepsilon\tau_{pm}}{2}\right)\Delta_{21}+$$
$$\left(\frac{\delta_1}{\sqrt{Q}}\right)\Delta_{22}+\delta_9$$

4.3 Piecewise linear desalting above salinity profile

For this case following Vidal and Acrivos (1966) ,

$$g(z)=\begin{cases}0, & 0\le z\le(1-\varepsilon)\\ \varepsilon^{-1}, & (1-\varepsilon)\le z\le 1\end{cases},$$
$$g_m(z_m)=\begin{cases}0, & 0\le z_m\le(1-\varepsilon_m)\\ \varepsilon_m^{-1}, & (1-\varepsilon_m)\le z_m\le 1\end{cases}$$

For this profile, the critical Rayleigh number is established from (4.17) and is accessed as $R_{c5}=\frac{\kappa\,\Delta_{37}}{\hat{T}\,\Delta_{38}}$ where, $\Delta's$ and $\delta's$ are given by

$$\delta_1=\frac{1}{2}\left(1+\frac{\tau_{pm}}{\varepsilon}\left(1-(1-\varepsilon)^2\right)\right),$$
$$\delta_8=\frac{1}{3}\left(1+\frac{\tau}{\varepsilon_m}\left(1-(1-\varepsilon_m)^3\right)\right),$$
$$\delta_2=\frac{1}{\sqrt{Q}}\left(sinh\sqrt{Q}+\frac{\tau_{pm}\delta_{21}}{\varepsilon}\right),$$
$$\delta_{21}=sinh\sqrt{Q}-sinh\left(\sqrt{Q}(1-\varepsilon)\right),$$
$$\delta_3=\frac{1}{\sqrt{Q}}\left(cosh\sqrt{Q}-1+\frac{\tau_{pm}\delta_{31}}{\varepsilon}\right),$$
$$\delta_{31}=\left(cosh\sqrt{Q}-cosh\left(\sqrt{Q}(1-\varepsilon)\right)\right),$$
$$\delta_4=\frac{1}{3}\left(1+\frac{\tau_{pm}}{\varepsilon}\left(1-(1-\varepsilon)^3\right)\right),$$
$$\delta_5=\frac{1}{2}\left(1+\frac{\tau}{\varepsilon_m}\left(1-(1-\varepsilon_m)^2\right)\right),$$
$$\delta_6=\frac{1}{\zeta}\left(sinh\zeta-sinh(\zeta(1-\varepsilon_m))\right),$$
$$\delta_7=\frac{1}{\zeta}\left(cosh\zeta-1+\frac{\tau}{\varepsilon_m}\right),$$
$$\delta_{71}=Cosh\zeta-Cosh(\zeta(1-\varepsilon_m)),$$
$$\delta_{81}=\hat{d}^2(\delta_6-1-\tau)\Delta_{16}+\hat{d}^2(\delta_7-\zeta\delta_5)\Delta_{17}-$$
$$\hat{d}^2\delta_8,$$
$$\delta_9=\hat{d}^2(\delta_6-1-\tau)\Delta_{18}+\hat{d}^2(\delta_7-\zeta\delta_5)\Delta_{19},$$
$$\delta_{10}=\hat{d}^2(\delta_6-1-\tau)\Delta_{14}+\hat{d}^2(\delta_7-\zeta\delta_5)\Delta_{15},$$
$$\Delta_{34}=(1+\tau_{pm})\Delta_{24}+\delta_1\Delta_{25}+\delta_2\Delta_{26}+$$
$$\delta_3\Delta_{27}+\delta_{81},$$
$$\Delta_{35}=(1+\tau_{pm})\Delta_{28}+\delta_1\Delta_{29}+\delta_2\Delta_{30}+$$
$$\delta_3\Delta_{31}-\delta_9,$$
$$\Delta_{36}=(1+\tau_{pm})\Delta_{20}+\delta_1\Delta_{21}+\delta_2\Delta_{22}+$$
$$\delta_3\Delta_{23}-\delta_4-\delta_{10}.$$

4.4 Piecewise linear step function salinity profile

In this salinity gradient the basic concentration drops instantly by ΔS at $z=\varepsilon$ and ΔS_m at $z_m=\varepsilon_m$ otherwise uniform. Accordingly, $g(z)=\delta(z-\varepsilon)$ and $g_m(z_m)=\delta(z_m-\varepsilon_m)$ where ε is the saline depth in region 1 and ε_m is the saline depth in the region 2. The critical Rayleigh number for this profile is obtained from (4.17) and is given by $R_{c6}=\frac{\kappa\,\Delta_{37}}{\hat{T}\,\Delta_{38}}$ where, $\Delta's$ and $\delta's$ are as below,

$$\delta_1=1+\tau_{pm},\quad \delta_2=\frac{1}{2}+\varepsilon\tau_{pm},$$
$$\delta_3=\frac{sinh\sqrt{Q}}{\sqrt{Q}}+\tau_{pm}cosh\varepsilon\sqrt{Q},$$
$$\delta_4=\frac{cosh\sqrt{Q}}{\sqrt{Q}}+\tau_{pm}sinh\varepsilon\sqrt{Q}-\frac{1}{\sqrt{Q}},$$
$$\delta_5=\frac{1}{3}+\tau_{pm}\varepsilon^2,\quad \delta_8=\frac{1}{3}+\tau\varepsilon_m^2$$
$$\delta_6=\frac{sinh\zeta}{\zeta}+\tau cosh\zeta\varepsilon_m-1-\tau,$$
$$\delta_7=\frac{cosh\zeta}{\zeta}+\tau sinh\zeta\varepsilon_m-\frac{1}{\zeta}-\frac{\zeta}{2}-\tau\zeta\varepsilon_m,$$
$$\Delta_{34}=\delta_1\Delta_{24}+\delta_2\Delta_{25}+\delta_3\Delta_{26}+\delta_4\Delta_{27}+$$
$$\hat{d}^2\delta_6\Delta_{16}+\hat{d}^2\delta_7\Delta_{17}-\hat{d}^2\delta_8,$$
$$\Delta_{35}=\delta_1\Delta_{28}+\delta_2\Delta_{29}+\delta_3\Delta_{30}+\delta_4\Delta_{31}-$$
$$\hat{d}^2\delta_6\Delta_{18}+\hat{d}^2\delta_7\Delta_{19},$$
$$\Delta_{36}=\delta_1\Delta_{20}+\delta_2\Delta_{21}+\delta_3\Delta_{22}+\delta_4\Delta_{23}-\delta_5-$$
$$\hat{d}^2\delta_6\Delta_{14}+\hat{d}^2\delta_7\Delta_{15}.$$

5. Graphical Interpretations

Figure 1 depicts the variations of thermal Rayleigh number R_c for Salting below, Desalting above and Step function profiles with respect to the ε for $Da = 0.01$, $\kappa = 1$, $\hat{d} = 5$, $\tau = 0.5$, $\tau_{pm} = 0.75$, $R_s = 10$, $M_s = 100$, $M = 10, \varepsilon_m = 0.75$, $\phi = 0.1$, $\hat{\mu} = 2.5$, $q = 5$, $\hat{S} = 1, \hat{T} = 1$.

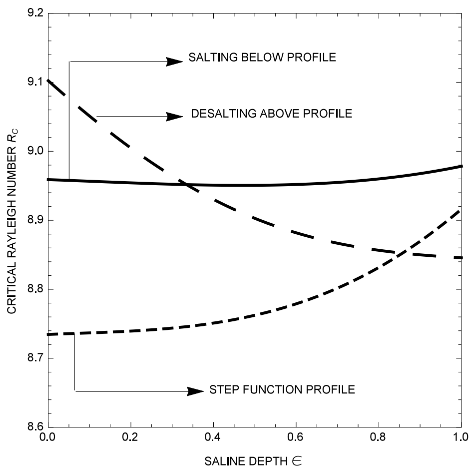

Figure 1. The variation of thermal Rayleigh number R_c for Salting below, Desalting above and Step function profiles with respect to the saline depth ε.

From the graph we have

Interval	Stable Profile	Unstable Profile
$0 \leq \varepsilon \leq 0.3$	Desalting above profile	Step function profile
$0.3 \leq \varepsilon \leq 0.85$	Salting below profile	Step function profile
$0.85 \leq \varepsilon \leq 1$	Salting below profile	Desalting above profile

By selecting the relevant salinity profile, the onset of double diffusive magneto – Marangoni convection in a composite layer can be restrained.

Figure 2 (a), (b) and (c) depicts the effects of $Da = 0.01$, $0.02, 0.03$ on R_c for Salting below, Desalting above and Step function salinity profiles with respect to the ε respectively, for $\kappa = 1$, $\hat{d} = 5$, $\tau = 0.5$, $\tau_{pm} = 0.75$, $R_s = 10$, $\hat{S} = 1$, $\hat{T} = 1$, $M_s = 100$, $M = 10$, $\varepsilon_m = 0.75$, $\phi = 0.1$, $\hat{\mu} = 2.5$, $q = 5$. The curves are converging for salting below and step function salinity profile showing that the effect is less for greater values of ε, also the curves are diverging for desalting above profile showing that the effect is larger as ε increases. For a constant value of ε, a small increase in Da decreases R_c, thus the system is destabilized and hence the onset of the convection is accelerated.

The effects of $\hat{d} = 5, 6, 7$ on R_c for Salting below, Desalting above and Step function profiles with respect to the ε

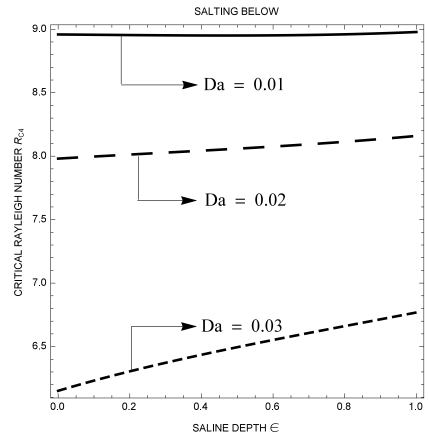

2a

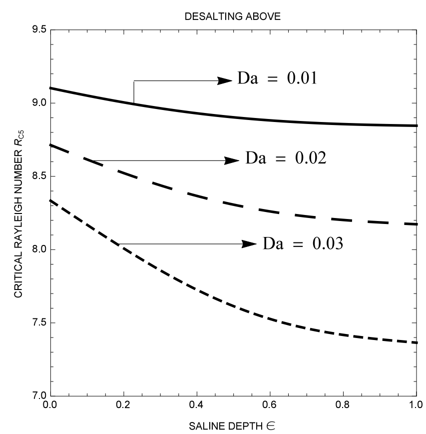

2b

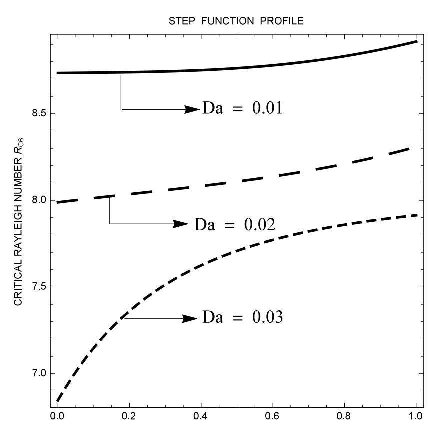

2c

Figure 2. The effect of Darcy number Da on critical thermal Rayleigh number R_c with respect to saline depth ε.

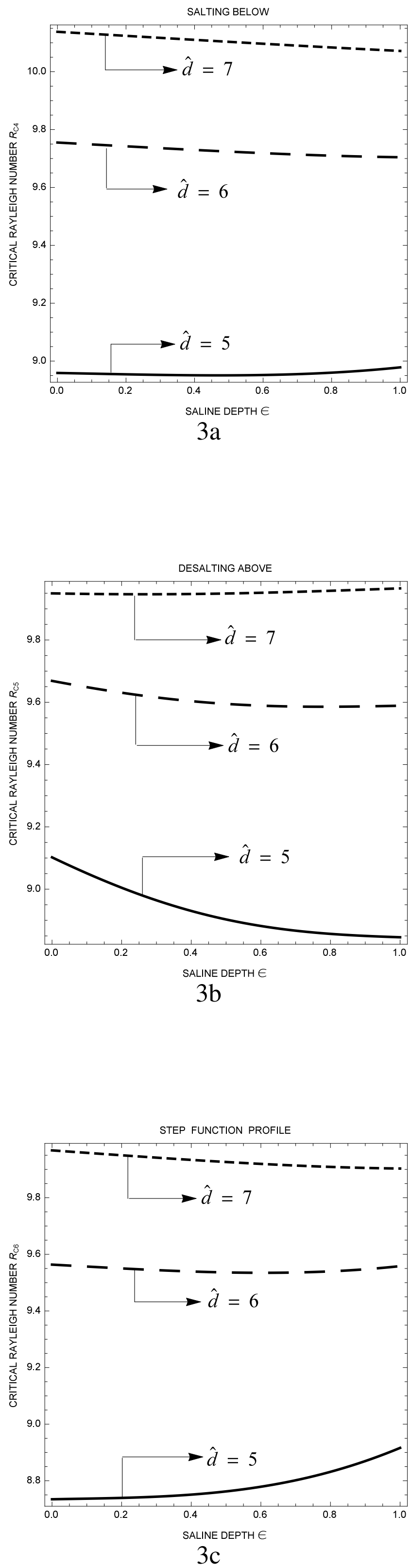

Figure 3. The effect of depth ratio $\hat{d}$ on critical thermal Rayleigh number R_c with respect to saline depth ε.

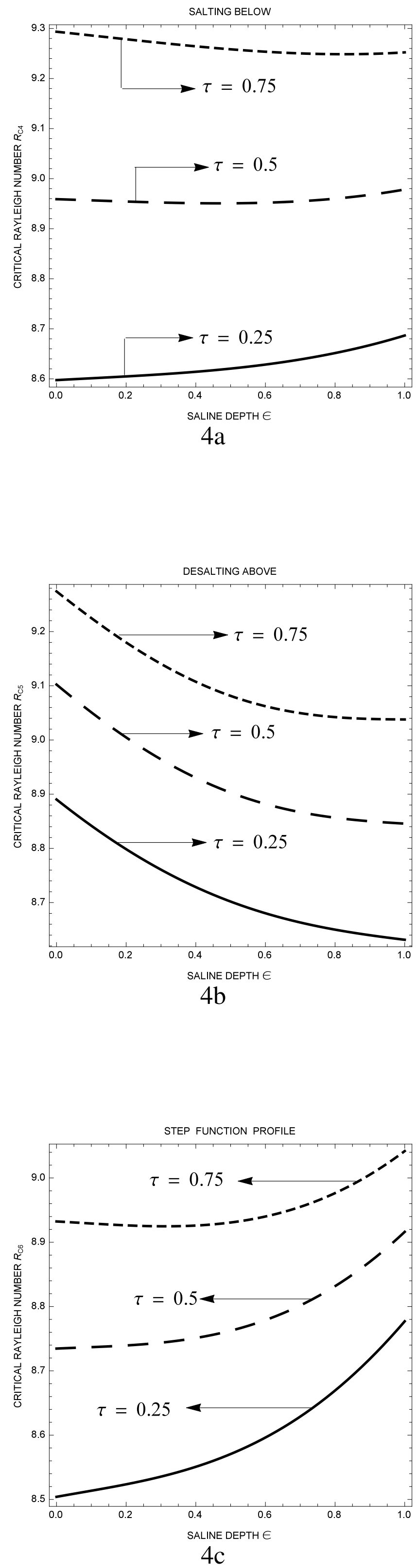

Figure 4. The effect of thermal diffusivity ratio τ on critical thermal Rayleigh number R_c with respect to saline depth ε.

are depicted in figures 3 (a), (b) and (c) respectively, for $\kappa = 1$, $Da = 0.01$, $\tau = 0.5$, $\tau_{pm} = 0.75$, $R_s = 10$, $\hat{S} = 1$, $\hat{T} = 1$, $M_s = 100$, $M = 10$, $\varepsilon_m = 0.75$, $\phi = 0.1$, $\hat{\mu} = 2.5$, $q = 5$. For a fixed ε, increase in $\hat{d}$ increases R_c, thus the system is stabilized and hence the onset of convection is postponed.

The effect of $\tau = 0.25, 0.5, 0.75$ on R_c for Salting below, Desalting above and Step function profiles with respect to ε are depicted in Figures 4 (a), (b) and (c) respectively, for $Da = 0.01$, $\kappa = 1$, $\hat{d} = 5$, $\tau_{pm} = 0.75$, $R_s = 10$, $M_s = 100$, $M = 10$, $\varepsilon_m = 0.75$, $\phi = 0.1$, $q = 5$, $\hat{S} = 1$, $\hat{T} = 1$. For a fixed ε, increase in τ increases R_c, thus the system is stabilized and hence the onset of the double diffusive magneto - Marangoni convection is postponed.

Conclusion

By increasing the Darcy number Da double diffusive magneto - Marangoni convection for all the above profiles is accelerated, which may be due to the presence of magnetic field. Also by increasing depth ratio $\hat{d}$ and thermal diffusivity ratio τ the onset of double diffusive magneto - Marangoni convection can be delayed for the above profiles.

References

[1] I.G. Currie, The effect of heating rate on the stability of stationary fluids, *Journal of Fluid Mechanics*, 29(1967), 337-347.

[2] F. Chen, C.F. Chen, A.J. Pearlstein, Convective instability in superposed fluid and anisotropic porous layers, *Phys. Fluids*, A3(4)(1991), 556–565.

[3] M. Hennenberg, M.Z. Saghir, A. Rednikov, J.C. Legros, Porous media and the Benard–Marangoni problem, *Transport Porous Med.*, 27(1997), 327–355.

[4] N. Rudraiah, V. Prasad, Effect of Brinkman boundary layer on the onset of Marangoni convection in a fluid saturated porous layer, *Acta Mech.*, 127 (1998), 235–246.

[5] D.A. Nield, Onset of Convection in a Fluid Layer overlying a layer of porous layer, *J. Fluid Mech.*, 1977, 513-522.

[6] J.R.A. Pearson, On Convection Cells induced by surface Tension, *J. Fluid Mech.*, 1958, 489-500.

[7] I.S. Shivakumara, S.P. Suma and K.B. Chavaraddi, Onset of surface-tension-driven convection in superposed layers of fluid and saturated porous medium, *Archives of Mechanics*, 58(2006), 71-92.

[8] I.S. Shivakumara, Jinho Lee and K.B. Chavaraddi, Onset of surface tension driven convection in a fluid layer overlying a layer of an anisotropic porous medium, *International Journal of Heat and Mass Transfer*, 54(2011), 994–1001.

[9] A. Vidal and A. Acrivos, Nature of the neutral state in surface tension driven convection, *Phys. Fluids*, 9(3)(1996), 615.

⋆⋆⋆⋆⋆⋆⋆⋆⋆
ISSN(P):2319 – 3786
Malaya Journal of Matematik
ISSN(O):2321 – 5666
⋆⋆⋆⋆⋆⋆⋆⋆⋆